Climatic Change
https://doi.org/10.1007/s10584-020-02944-7

Non-analog increases to air, surface, and belowground temperature extreme events due to climate change

M. D. Petrie[1] · J. B. Bradford[2] · W. K. Lauenroth[3] · D. R. Schlaepfer[2,3,4] · C. M. Andrews[2] · D. M. Bell[5]

Received: 20 May 2020 / Accepted: 5 November 2020 / Published online: 09 December 2020

Abstract
Air temperatures (Ta) are rising in a changing climate, increasing extreme temperature events. Examining how Ta increases are influencing extreme temperatures at the soil surface and belowground in the soil profile can refine our understanding of the ecological consequences of rising temperatures. In this paper, we validate surface and soil temperature (Ts: 0–100-cm depth) simulations in the SOILWAT2 model for 29 locations comprising 5 ecosystem types in the central and western USA. We determine the temperature characteristics of these locations from 1980 to 2015, and explore simulations of Ta and Ts change over 2030–2065 and 2065–2100 time periods using General Circulation Model (GCM) projections and the RCP 8.5 emissions scenario. We define temperature extremes using a nonstationary peak over threshold method, quantified from standard deviations above the mean (0-σ: an event $>\sim$ 51% of extreme events; 2-σ :$>\sim$ 98%). Our primary objective is to contrast the magnitude (°C) and frequency of occurrence of extreme temperature events between the twentieth and twenty-first century. We project that temperatures will increase substantially in the twenty-first century. Extreme Ta events will experience the largest increases by magnitude, and extreme Ts events will experience the largest increases by proportion. On average, 2-σ extreme Ts events will increase by 3.4 °C in 2030–2065 and by 5.3 °C in 2065–2100. Increases in extreme Ts events will often exceed +10 °C at 0–20 cm by 2065–2100, and at 0–100 cm will often exceed 5.0 standard deviations above 1980–2015 values. 2-σ extreme Ts events will increase from 0.9 events per decade in 1980–2015 to 23 events in 2030–2065 and 38 events in 2065–2100. By 2065–2100, the majority of months will experience extreme events that co-occur at 0–100 cm, which did not occur in 1980–2015. These projections illustrate the non-analog temperature increases that ecosystems will experience in the twenty-first century as a result of climate change.

Keywords Soil temperature · Air temperature · Extremes · Ecosystems

✉ M. D. Petrie
matthew.petrie@unlv.edu

Extended author information available on the last page of the article.

1 Introduction

Projections for increasing air temperatures (Ta: °C) are among the most robust and consistent of those made by General Circulation Models (GCMs) for scenarios of twenty-first century climate change (IPCC 2013). Increasing Ta is predicted to impact ecosystems through multiple pathways including increasing evaporative demand and increasing aridity (IPCC 2013; Gutzler and Robbins 2011), lengthening the growing season and altering phenology (Julien and Sobrino 2009; Petrie et al. 2015), and by changing the rate and magnitude of biological processes including ecosystem respiration and nutrient cycling (Yuste et al. 2007; Hamdi et al. 2013). Increasing Ta and extreme Ta events are already being observed and attributed to climate change (King et al. 2016), and predicting their future patterns and impacts is the subject of research in many ecosystems (see Betts et al. 2000 and Selig et al. 2010 for examples). Of future climate changes, temperature change at the land surface and belowground in the soil profile (Ts: °C) has been documented at multiple locations over the past 20 years (Garcia-Suarez and Butler 2006; Qian et al. 2011; Svilicic et al. 2016). The ecological impacts of these increases are less understood, especially those resulting from extreme Ts events. Thus, Ts change is a major knowledge gap that increases uncertainty of future climate change impacts to ecosystems.

Recent observations of increasing temperature effects on ecosystems include declines in coniferous forests across western North America (Williams et al. 2013), earlier growing season onset leading to increased plant vulnerability to freezing (Wheeler et al. 2014), reduced efficiency of plant gas exchange and evaporative cooling (Noia Junior et al. 2018), and exceedance of species' thermal tolerance limits (O'Sullivan et al. 2017). In contrast, Collins et al. (2017) and Ratajczak et al. (2019) found that grassland communities in the Chihuahuan Desert and central Great Plains, respectively, were only responsive to multiple global change drivers, including enhanced temperatures, when they co-occurred with other disturbances. These divergent findings underscore the need to better understand the role that belowground temperatures play on ecological processes, and to identify the characteristics of ecosystems that will shape their sensitivity to future Ts changes. As an additional component of temperature change, climate-driven extreme events are in many cases more meaningful for biological processes than change to mean conditions are (Katz and Brown 1992). We postulate that Ts extremes may therefore be an underrecognized component of extreme climate events and may have ecological impacts that have previously been attributed to other climate variables (Barron-Gafford et al. 2012; Bradford et al. 2014a).

Of potential ecological impacts, predictions for increasing global temperatures to alter belowground rates of biological functioning are of high concern (Darrouzet-Nardi et al. 2015; Alster et al. 2020). Soil microbial activity and heterotrophic soil respiration have been found to decline with elevated Ts in some ecological regions and increase in others, leading to unknown and potentially divergent impacts if these changes occur across broad regions (Hamdi et al. 2013; Bradford et al. 2016). Declines in belowground biological mobilization of plant available soil nutrients would have severe impacts to arid and semiarid (dryland) ecosystems, and could potentially lead to a decline in net primary production and a shift in ecosystem carbon budget towards more years of net carbon loss (Belnap 2002; Rudgers et al. 2018). Belowground rates of biological functioning are also associated with soil water infiltration and plant photosynthesis (Whitney et al. 2017; Rudgers et al. 2018), as well as increased soil stability for vegetation persistence and expansion (Rodriguez-Caballero et al. 2018; Chung et al. 2019). Although the extent of temperature-driven declines in belowground biological functioning is still being elucidated, these declines could constitute an additional stress agent to many ecosystems, and may be an important mechanism that

shapes global ecological trends in species range shifts, deterioration and desertification, and ecological state transitions (D'Odorico et al. 2013; Bell et al. 2014).

In contrast to changes in rainfall—the detailed properties (mean, variation, extremes) of which are the subject of substantial ecological research—temperature change is often simplified as a factor that is regulated by moisture availability. Research focusing on extreme precipitation- and temperature-driven events such as hot-drought and heat pulses are a good example of this focus, and provide a useful framework for understanding multifactor climate change impacts to ecosystems, agriculture, and human health (Bradford et al. 2017; Mora et al. 2017). Yet, this focus on multifactor effects may fail to identify independent effects of increasing temperatures, especially those associated with change to Ts. We propose that the current gap in understanding Ts impacts to ecosystems can begin to be addressed by insight in two areas: (1) Detailed characterization of change to the properties of Ta and Ts extreme events in scenarios of climate change; and (2) Better understanding of how increasing extreme Ts events at the land surface (Ts: 0-cm depth) and belowground (Ts: 1+ cm) are influenced by increasing Ta. The way that climate extremes influence ecological processes across multiple levels of spatial organization (belowground to atmospheric linkages, local to regional spatial scales) is becoming more clear (Diffenbaugh et al. 2005; Reichstein et al. 2013), and Ts extremes may be an important, but largely unrecognized, component of these processes.

There are a number of plausible reasons explaining why Ts extremes have received less attention than Ta extremes. First, continuous, long-term measurements of Ts have not yet been sustained for sufficient time periods to observe a large number of belowground extreme events, making their attribution to observed ecological responses difficult compared to aboveground events (Moran et al. 2008). Even at a single location, the time and costs of field campaigns and infrastructure to continuously measure aboveground and belowground variables are prohibitive and may only capture a small number of extreme events. Furthermore, it is impossible to both measure belowground dynamics (such as Ts) and characterize belowground conditions (such as soil texture) at the exact same location because soils must be destructively sampled to be characterized. It is also presumable that Ts extremes have not been prioritized because temperature propagation belowground is dampened by the high thermal inertia of soil, such that extreme events do not occur or that they may not be ecologically-meaningful (Eitzinger et al. 2000). Field experiments that manipulate belowground temperatures are also relatively rare (see Yuste et al. 2007 and Noia Junior et al. 2018 for exceptions), and it is difficult to attribute belowground measurements to ecological processes even in an experimental setting. Thus, although there has been evidence for some time that Ts patterns and extreme Ts events impact ecosystems, the number of identified Ts impacts remains relatively low.

By examining how Ta increases are influencing extreme temperatures at the soil surface and belowground in the soil profile that control ecosystem dynamics, we can refine our understanding of the ecological consequences of rising temperatures. In this study, we used the SOILWAT2 model to contrast patterns in the magnitude (°C), frequency of occurrence (events 10 year^{-1}) and distribution (proportion of events in different classifications) of Ta and Ts extremes between historical time periods (1980–2015), and projections of twenty-first century climate change for two time periods (2030–2065, 2066–2100) for mesic and semiarid ecosystems in the central and western USA. We were specifically interested in the maximum of extreme temperatures occurring during the April–October growing season. Our objectives were to (1) identify the primary climatic and landscape factors shaping Ts; (2) contrast expected increases in the magnitude and occurrence of extreme Ts events to expected increases in the magnitude and occurrence of extreme Ta events in the

twenty-first century; and (3) determine how the frequency of Ts events considered "extreme" by historical standards will change in the future, and over what timescales and depths in the soil profile these changes will occur. Because Ta is mechanistically linked to Ts, we tested the hypothesis that land surface and soil factors shaping the belowground propagation of temperature through the soil profile reduce the frequency and magnitude of extreme Ts events, but that rising temperatures will increase correlation between extreme Ta and Ts events in the future. Forecasts of extreme Ta and Ts events offer new insight on the suite of climate-associated changes that ecosystems will experience in coming decades and will help to sharpen research that seeks to identify the ecological consequences of these changes.

2 Site description

We forecast Ta and Ts extremes for 29 locations comprising 5 broad ecosystem classes in the central and western USA: desert grasslands and shrublands (Desert: 3 locations), semiarid grasslands and shrublands (Semiarid: 8 locations), mesic grasslands (Mesic: 4 locations), woodlands and shrublands (Wood-shrub: 8 locations), and coniferous forests (Forest: 6 locations; Table 1, Fig. 1). We chose locations to span a broad range of climate conditions, vegetation communities, aboveground biomass, soil properties, and site characteristics (Table 1). The factors across which these locations vary can all influence belowground temperature propagation, but we note that they lack the within-ecosystem diversity needed to elucidate how these factors shape temperature across finer levels of landscape and vegetation heterogeneity. From 1980 to 2015 (36 years at each location), average annual precipitation (P: mm) ranged from an average low of 81 mm (Desert: NV 53136) to a high of 2781 mm (Forest: WA Wrc; Table 1). Ta was higher in southern compared to northern locations, although elevation also shaped these values (Table 1). Soil depth was highest at Mesic locations, often reaching depths $>$ 150 cm, and was lowest in Desert and Wood-shrub locations, in one case $<$100 cm (Wood-shrub: NM Spj) (Soil Survey Staff 2016).

3 Methods

3.1 Site selection, field data, and field data filtering

Our study locations had multiple years of P, Ta, and Ts data. The majority of these locations (22) were part of the National Oceanic and Atmospheric Administration (NOAA) United States Climate Reference Network (USCRN), and were instrumented identically (https://www.ncdc.noaa.gov/crn/). Most USCRN locations had Ts data available at four depths: 5 cm, 20 cm, 50 cm, and 100 cm, and we used data from 2010 to 2014 for these locations when available. Because USCRN forest locations were not located within a forest canopy, we obtained within-canopy meteorological and Ts data for six forests from the Ameriflux Network (http://ameriflux.ornl.gov/). These locations were comprised of open- and closed-canopy coniferous forests dominated by species including ponderosa pine, Douglas fir, and western Hemlock (Table 1). We also added an additional piñon pine and juniper-dominated location from the Sevilleta Long-Term Ecological Research (LTER) Network (NM Spj) (http://sev.lternet.edu/). Data range, measurement depths, and instrumentation at the Ameriflux and LTER locations differed from those of USCRN locations, but their

Table 1 Site characteristics and variables influencing belowground temperature, averaged for 0–100-cm soil depths. Biomass values are combined near-surface living plant biomass, dead plant biomass, and litter. Values in italics indicate the mean and standard deviation of site characteristics and variables for each ecosystem type

Site ID	Ecosystem type	Ecosystem classification	Elevation (mm)	MAP (cm)	MAT (°C)	Biomass (g m^{-2})	Sand (%)	% Clay (%)	Bulk density (g cm^{-3})	Thermal conductivity (w $m^{-1} \cdot K$)	Heat capacity (J $m^{-3} \cdot K$)
NM 03048	Desert	Grassland	1477	169	15.3	308	49	4	1.76	$7.2e^{-4}$	0.23
NM 03074	Desert	Shrubland	1319	174	15.7	278	37	19	1.83	$7.8e^{-4}$	0.25
NV 53136	Desert	Shrubland	1001	81	18.1	395	22	1	1.83	$7.1e^{-4}$	0.21
Mean			*1266 ± 242*	*141 ± 52*	*16.4 ± 1.5*	*327 ± 61*	*36 ± 14*	*8 ± 10*	*1.81 ± 0.04*	*$7.1e^{-4}$ ± $0.4e^{-4}$*	*0.23 ± 0.02*
CO 03063	Semiarid	Grassland	1337	237	12.4	338	16	13	1.64	$8.2e^{-4}$	0.30
CO 94074	Semiarid	Grassland	1643	331	9.3	301	17	5	1.79	$7.4e^{-4}$	0.25
MT 04140	Semiarid	Grassland	1545	443	5.8	360	13	11	1.66	$9.0e^{-4}$	0.32
ND 94084	Semiarid	Grassland	561	479	3.7	332	27	20	1.72	$9.0e^{-4}$	0.37
OR 04125	Semiarid	Grassland	684	227	12.2	418	18	31	1.86	$7.7e^{-4}$	0.26
TX 03054	Semiarid	Grassland	1141	319	15.5	391	31	15	1.67	$7.5e^{-4}$	0.29
WA 04136	Semiarid	Grassland	691	446	8.0	551	18	9	1.74	$8.1e^{-4}$	0.30
WY 94088	Semiarid	Grassland	1765	786	5.8	578	28	17	1.73	$9.0e^{-4}$	0.43
Mean			*1171 ± 476*	*409 ± 180*	*9.1 ± 4.0*	*409 ± 103*	*21 ± 7*	*15 ± 8*	*1.73 ± 0.07*	*$8.2e^{-4}$± $0.7e^{-4}$*	*0.32 ± 0.06*
IA 54902	Mesic	Grassland	281	849	10.4	603	5	30	1.45	$8.9e^{-4}$	0.46
IL 54808	Mesic	Grassland	213	899	11.2	650	7	25	1.52	$8.1e^{-4}$	0.36
NE 94996	Mesic	Grassland	418	691	11.6	490	21	26	1.57	$8.5e^{-4}$	0.42
SD 04990	Mesic	Grassland	486	662	7.9	465	54	10	1.65	$8.6e^{-4}$	0.43
Mean			*350 ± 125*	*775 ± 116*	*10.3 ± 1.7*	*552 ± 89*	*22 ± 23*	*23 ± 9*	*1.55 ± 0.08*	*$8.5e^{-4}$ ± $0.3e^{-4}$*	*0.42 ± 0.04*
CA 04222	Woodland	Coastal	432	976	16.3	350	32	9	1.77	$7.5e^{-4}$	0.25
CA 53150	Woodland	Coastal	2018	837	10.4	350	13	6	1.72	$7.6e^{-4}$	0.23
CO 03061	Woodland	Juniper	2449	388	9.1	1225	26	19	1.73	$7.9e^{-4}$	0.32

Table 1 (continued)

Site ID	Ecosystem type	Ecosystem classification	Elevation (mm)	MAP (cm)	MAT (°C)	Biomass (g m^{-2})	Sand (%)	% Clay (%)	Bulk density (g cm^{-3})	Thermal conductivity (w $m^{-1} \cdot K$)	Heat capacity (J $m^{-3} \cdot K$)
NM Pj	Woodland	Pinon-juniper	1911	281	13.0	1225	33	5	2.04	$7.3e^{-4}$	0.21
CO 03060	Shrubland	Sagebrush	2561	501	6.4	528	30	39	1.56	$8.4e^{-4}$	0.37
ID 04127	Shrubland	Sagebrush	1204	268	10.0	453	22	16	1.74	$7.4e^{-4}$	0.30
OR 04128	Shrubland	Sagebrush	1397	224	8.2	387	27	23	1.60	$7.7e^{-4}$	0.31
UT 04138	Shrubland	Sagebrush	1509	283	9.5	458	21	12	1.69	$8.6e^{-4}$	0.39
Mean			*1685 ± 700*	*470 ± 286*	*10.4 ± 3.1*	*622 ± 377*	*26 ± 7*	*16 ± 11*	*1.73 ± 0.14*	*$7.8e^{-4} \pm 0.5e^{-4}$*	*0.30 ± 0.06*
AZ Fmf	Forest	Ponderosa	2160	524	9.7	1319	19	32	1.57	$8.5e^{-4}$	0.27
CA Blo	Forest	Ponderosa	1315	1401	11.2	1319	25	19	1.81	$7.8e^{-4}$	0.25
OR Me2	Forest	Ponderosa	1253	590	7.3	1147	13	4	1.68	$8.4e^{-4}$	0.36
OR Mrf	Forest	Spruce	263	1243	9.6	1147	8	28	1.48	$8.2e^{-4}$	0.33
WA Wrc	Forest	Spruce	371	2781	9.4	1780	43	13	1.71	$8.4e^{-4}$	0.39
WY Gle	Forest	Spruce	3190	1464	−0.2	6965	38	12	1.65	$8.9e^{-4}$	0.42
Mean			*1425 ± 1110*	*1334 ± 817*	*7.8 ± 4.1*	*2280 ± 2307*	*24 ± 14*	*18 ± 11*	*1.65 ± 0.11*	*$8.4e^{-4} \pm 0.4e^{-4}$*	*0.34 ± 0.07*

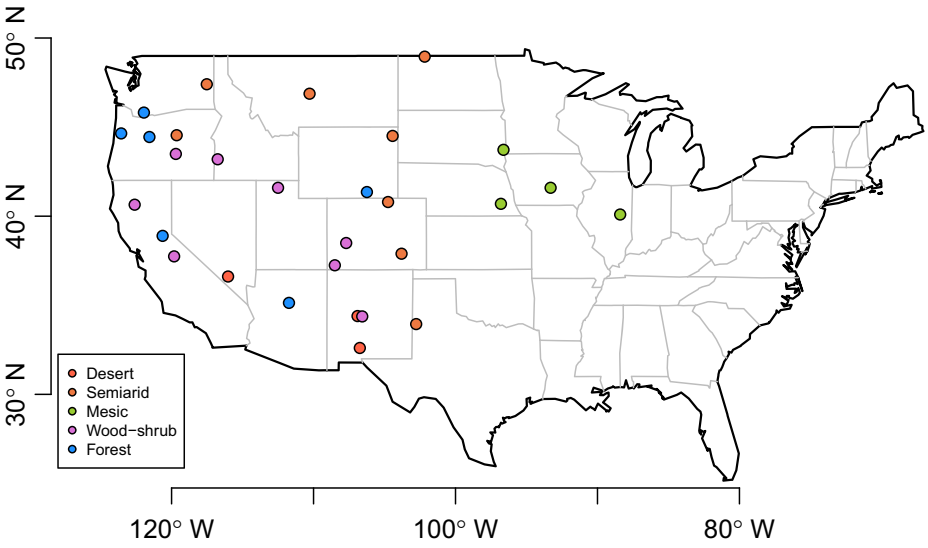

Fig. 1 Site locations and ecosystem type

inclusion enabled us to include additional ecosystems in our study. We removed erroneous and flagged Ta and Ts data for each site, and resulting gaps were $< 0.7\%$ of total observations, with the exception of AZ-Fmf and CA-Blo which were $\sim 5.0\%$. We compiled Ta and Ts data to daily averages, and gapfilled Ta using MicroMet preprocessor and moving-average time series model methodologies (Henn et al. 2013). We did not gapfill Ts data, and limited our analysis to days when these data were available, and to days when upper soil layers were unfrozen (mean daily Ts > 2 °C).

3.2 SOILWAT2 parameters and simulation

We simulated daily values of Ts from 0 to 100 cm using the SOILWAT2 model (Schlaepfer and Andrews 2019; Schlaepfer and Murphy 2019). SOILWAT2 is a daily time step, one-dimensional, multiple soil layer, process-based, water balance simulation model. The model translates meteorological conditions from observations and spatial data products into a full suite of ecosystem water balance processes as well as Ts. We estimated parameters for the meteorology of each study location (cloud cover, wind speed, solar radiation) using monthly National Oceanic and Atmospheric Administration, National Centers for Environmental Information Climate Atlas data (https://www.ncdc.noaa.gov/climate-information/climate-us). For Desert, Semiarid, Mesic, and Wood-shrub locations, we estimated vegetation composition, aboveground biomass, and phenology from Bradford et al. (2014b), and estimated these parameters for Forest locations using averages from the nearest three United States Department of Agriculture Forest Service Forest Inventory Analysis (FIA) sites (http://www.fia.fs.fed.us/). We estimated parameters for soil characteristics at each location (% gravel, % sand, % clay) using gridded United States Department of Agriculture, Natural Resources Conservation Service STATSGO data (http://water.usgs.gov/GIS/metadata/usgswrd/XML/ussoils.xml).

We compiled meteorological conditions used to drive SOILWAT2 from historical climate observations and downscaled future climate forecasts implemented across regionally

appropriate general circulation models (GCMs). Simulations from 1980 to 2015 were driven using a 1/8-degree gridded climate product (Maurer et al. 2002). Values from 2030–2065 to 2066–2100 were developed from independent simulations across 11 GCMs using the RCP 8.5 emissions scenario (CMIP5; Maurer et al. 2007). We used a hybrid-delta downscaling approach to generate daily weather projections from GCMs required to drive SOILWAT2 (Tohver et al. 2014), a workflow that has been demonstrated in several previous studies (Petrie et al. 2017; Schlaepfer et al. 2017; Bradford and Bell 2017). GCMs were selected to represent the most independent (Knutti et al. 2013) and best performing (Rupp et al. 2013) subset of GCMs for the western USA. To represent diversity in GCM projections, our analysis focuses on GCM results based on the magnitude of future Ta projections. These include the median of the 11 GCMs (CESM1-CAM5: median) and also include results from the median of the 3 models with the highest future Ta projections (IPSL-CM5A-MR: high), and from the median of the 3 models with the lowest future Ta projections (inmcm4: low).

To compare SOILWAT2-predicted versus field observed values of Ts from 5 to 100 cm, we used a modified version of Mielke's r from Duveiller et al. (2015), which reduces the r correlation coefficient in response to additive and multiplicative biases, instead of major-axis regressions or slope-intercept techniques, which are less-adept at accounting for these biases. We calculated root mean square error (RMSE) between observed and predicted values to provide an easily-interpretable estimate of error in Ts. We plotted observed (y-axis) versus simulated (x-axis) values based on the findings of Pineiro et al. (2008). We used 5-day floating mean temperature values for our analysis, which provided the best parity between observation number and model fit. Across soil depths from 5 to 100 cm, April–October values of Mielke's r ranged from 0.85 to 0.99 and RMSE ranged from 0.91 to 3.26 °C (Supplementary Table 1, Supplementary Fig. 1). Field data were only used for model validation and were not included in our analyses.

3.3 Analysis

We contrasted patterns in Ta and Ts between 1980 and 2015 and projections of future climate change for the months of April–October for 2030–2065 and 2065–2100. This analysis uses the peak over threshold (POT) technique of Coelho et al. (2008) for daily temperature values, which identifies extremes based on the distribution of observed daily values that occur above a floating mean value (L-value), such that a month with $\geq$20 daily values above the floating mean will have one or more daily values above the 95th percentile from all values from that month, and therefore has one or more daily values that are statistically extreme (Fig. 2a; see Appendix for a review). The highest observed or simulated daily value below the 95th percentile is the extreme threshold value (°C), which constitutes the boundary between events above and below the 95th percentile (U-value; Fig. 2a). We focused our analyses on the magnitude and distribution of extreme threshold values, which captures monthly temperature extremes without focusing on the magnitude of a few number of simulated events, which are highly uncertain. This statistical determination of extreme events by POT differs from colloquial definitions of "extreme events," but is a robust analysis of high temperature patterns that is nonstationary (e.g., extreme events are shaped by above-average temperature values across a 5-year floating mean), and is often very similar in magnitude to events above the threshold (Fig. 2a).

We calculated the extreme threshold value (U-value) at each of our 29 study locations in each month using 5-day floating mean (target day $\pm$ 2 days) values for each temperature variable (Ta, Ts 0–100 cm), which corresponds to the time window of best fit in the SOILWAT2 model. In previous testing of this method, we determined that relatively short

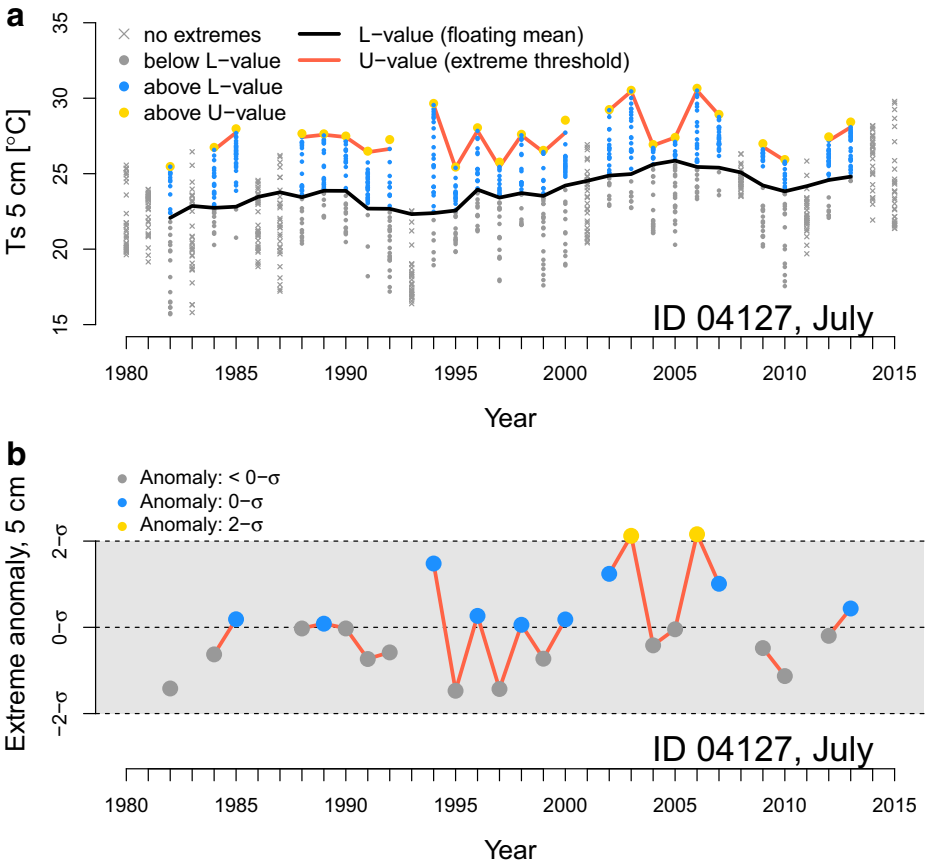

Fig. 2 Example calculation of the monthly extreme threshold value at 5 cm soil depth for a single location (ID 04127) in July from 1980 to 2015 (panel a), and analysis of the extreme threshold anomaly (<0-σ, 0-σ, 2-σ) over this time period (panel b)

floating mean values can be used accurately and also maximize the time period of analysis, and we therefore calculated a 5-year floating mean (L-value; target year $\pm$ 2 years) for each temperature variable in each month independently, and calculated an extreme threshold for each month when $\geq$20 values above the 5-year floating mean occurred. If <20 daily values above the floating mean occurred, there was no extreme threshold value in that particular month and therefore no extreme event. This analysis allows for a different threshold value in each month (April–October), and a maximum of 70 extreme events per decade. We refer to months with an extreme threshold value as having experienced an extreme temperate (Ta, Ts) event (Fig. 2a).

Because the POT technique identifies extreme events in many months, we further categorized these events by calculating their anomaly from the long-term mean and standard deviation of extreme threshold values (Anomaly $= \frac{\text{observed}-\text{mean}}{\text{std.dev.}}$). A 0-$\sigma$ anomaly corresponds and extreme threshold $>$ the mean and <2 standard deviations above the mean, and designates a median extreme event. Across the locations of our study, these events were higher than $\sim$ 51% of extreme events (Fig. 2b, Supplementary Fig. 2, Supplementary Table 2). A 2-σ anomaly corresponds to unusually high extreme thresholds $\geq$2 standard

deviations above the mean and was higher than ~ 98% of extreme events (Fig. 2b, Supplementary Figs. 2, 3, Supplementary Table 2). 0-σ and 2-σ extreme events were analyzed separately in our analyses (e.g., 2-σ were not part of the 0-σ).

This research focuses on contrasting extreme events between twenty-first century time periods (2030–2065, 2065–2100) and one historical time period (1980–2015). We did this in two ways: (method 1) By comparing the properties of extreme events within each time period, which provides a measure of the increasing magnitude of future events but maintains a similar frequency; and (method 2) By calculating extreme event anomalies (0-σ, 2-σ) in future time periods (2030–2065, 2065–2100) using the historical mean and standard deviation of extreme events in the past (1980–2015). This provides an estimate of the changing distribution of extreme events and of the changing frequency of months with a 0-σ or 2-σ extreme event (e.g. the changing occurrence of 0-σ and 2-σ extreme events in the future, based on past events). Our analysis focused on 3 types of extreme event anomalies: (1) Anomalies in 1980–2015 that were calculated from the 1980 to 2015 mean and standard deviation (providing baseline values for analysis of future patterns); (2) Anomalies in 2030–2065 and 2065–2100 that were calculated from the mean and standard deviation of values within each corresponding time period (method 1 above); and (3) Anomalies in 2030–2065 and 2065–2100 that were calculated from the mean and standard deviation of extreme events in 1980–2015 (method 2 above). Our analyses were generated from data for each study location (Table 1) and from SOILWAT2 simulations, and were conducted using R-package statistical computing software (R Development Core Team 2019).

3.4 Determination of factors influencing soil temperatures

We used a multimodel comparison analysis (Akaike information criterion (AIC)) to better understand the factors shaping Ts patterns across our 5 broad ecosystem types. AIC provides a measure of relative quality across linear models and maintains transferability between models (Chatfield 1995; Sarle 1995) by penalizing model complexity and the inclusion of covarying predictor variables (Burnham and Anderson 2002, 2004; Wenger and Olden 2012). We developed a set of orthogonal surface and soil variables for each ecosystem type, and refined this set to a group of 5 explanatory variables with R^2 <0.32. Variables included 5-day average maximum Ta (Ta max: °C), aboveground living and dead plant biomass (g m^{-2}), soil clay content from 0 to 100 cm (%), soil bulk density from 0 to 100 cm (g cm^{-3}), and soil thermal conductivity from 0 to 100 cm (w $m^{-1} \cdot K$). Although these soil variables have some interactive potential (soil clay content is a component of bulk density, for example), we expected that these interactions were low, and we did not observe nonlinear significant relationships ($R^2 \geq 0.4$) between these variables. Our univariate AIC analysis identified the dominant linear model explaining variation in Ts for different ecosystem types. To better identify the linear models that had a sub-dominant influence on Ts, we removed the top variable for our multivariate analysis.

4 Results

4.1 Factors influencing soil temperatures: 1980–2015

Maximum air temperature (Ta max) was the best univariate predictor of Ts from 5 to 100-cm depth for all ecosystem types in our study (Supplementary Table 3). Multivariate predic-

tors included aboveground biomass (Desert, Wood-shrub, Forest), as well as physical soil characteristics including soil clay content (Desert, Semiarid, Mesic), bulk density (Semiarid, Mesic, Wood-shrub, Forest), and thermal conductivity (Semiarid, Mesic, Wood-shrub, Forest; Supplementary Table 3). AIC results capture the factors associated with differences between the locations in each ecosystem type and do not necessarily capture the relative influence of these factors to Ts patterns at each individual location. Thus, although local variation in landscape factors (biomass, soils, etc.) impart differences in the propagation of Ts in the soil profile, Ts is most strongly associated with Ta max across all of our study locations. Based on this result, we use Ta max to present change to Ta in all of our analyses (Ta max = Ta hereafter).

4.2 Ta and Ts extreme events: 1980–2015

Extreme Ta and Ts events occurred from 1980 to 2015 across all locations. Extreme events were of the highest magnitude above (Ta) and near the soil surface (0–5 cm) and declined from 0 to 100 cm (Fig. 3; Supplementary Table 4). 0-σ and 2-σ extreme Ts events occurred at frequencies of $\sim$ 22–29 and $\sim$ 0–1.4 events per decade, respectively (Supplementary Table 4). Extreme Ts events did not usually occur at lower soil depths (50–100 cm) due to low Ts variation in these soil layers, and therefore few values above the floating mean (Fig. 3e, f). Co-occurrence of extreme Ts events at multiple soil depths in the same month was infrequent; $\sim$ 53% of months experienced fewer than 2 0-σ events, and $\sim$ 98% of months experienced fewer than 2 2-σ events (Fig. 4). That is, when a 0-σ or 2-σ Ts extreme event occurred, it was uncommon for another extreme event to co-occur at any other depth in the soil profile.

4.3 Method 1: Ta and Ts extreme events by magnitude: 2030–2065 and 2065–2100

Projections from the median GCM show that the temperature designating 0-σ extreme Ta events will increase substantially in the coming century (2030–2065: +5.2–6.8 °C; 2065–2100: +7.3–9.7 °C; Fig. 3, Supplementary Tables 5, 6). 2-σ extreme Ta events will experience even greater increases (2030–2065: +6.1–8.8 °C; 2065–2100: +8.5–11.4 °C; Fig. 3, Supplementary Tables 5, 6). Compared to Ta, extremes Ts events will experience lower increases (0-σ in 2030–2065/2065–2100: +3.9 °C/+5.8 °C; 2-σ in 2030–2065/2065–2100: +3.4 °C/+5.3 °C; Fig. 3). Across low, median, and high GCMs, extreme Ts events will consistently exceed the historical range of variability by as many as 5–15 standard deviations above the 1980–2015 mean (Fig. 5). Generally, the largest increases in the magnitude of extreme Ts events will occur in Deserts and at shallower soil depths (0–20 cm; Fig. 3), whereas the largest increases by anomaly (e.g., proportional increases) will occur at cooler ecosystem types (Semiarid, Mesic, Forest) and at deeper soil depths (50–100 cm; Fig. 5).

4.4 Method 2: Ta and Ts extreme events by occurrence (distribution and frequency): 2030–2065 and 2065–2100

Projections from the median GCM show that the frequency of months with extreme Ta and Ts events will increase in the future. In general, increasing temperatures will lead to a decline in the frequency of months experiencing a 0-σ extreme event, and a commensurate increase in the frequency of months experiencing a 2-σ extreme event (Fig. 6).

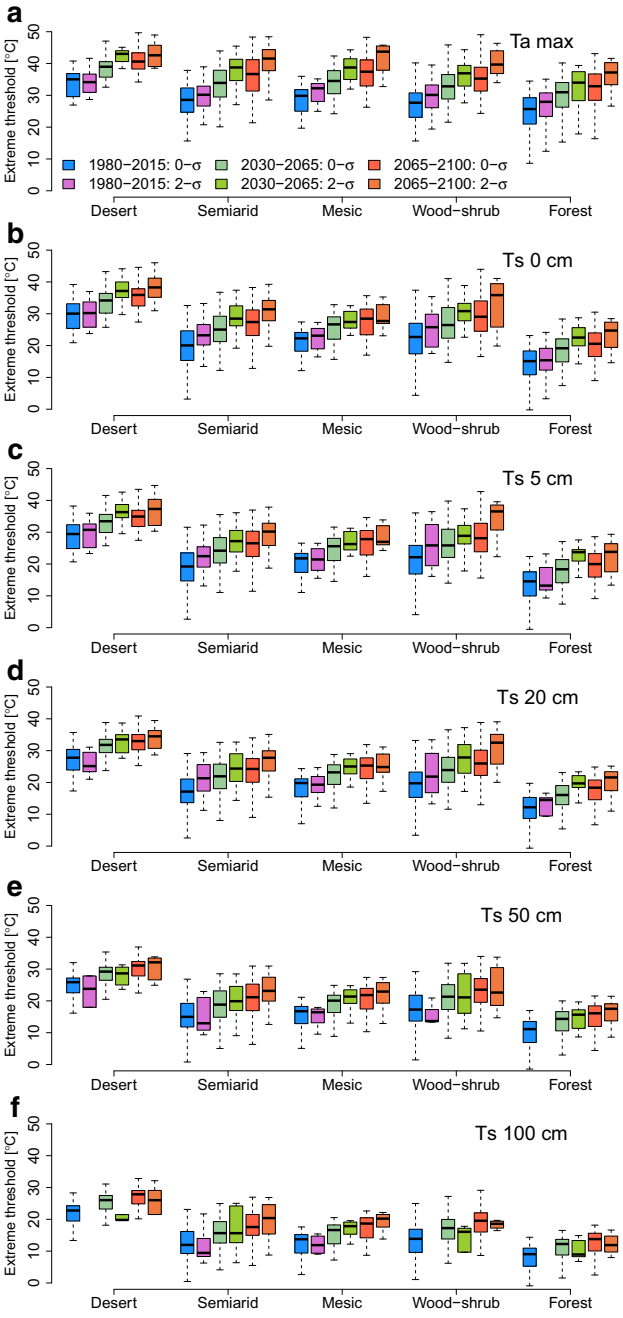

Fig. 3 Boxplots illustrating the magnitude (°C) of months corresponding to 0-σ and 2-σ extreme events between 1980–2015, 2030–2065, and 2065–2100 (future values from CESM-CAM5: the median of all 11 models). Extreme events are summarized for maximum air temperature (Ta max, panel a) and soil temperatures (0–100-cm depth, panels b–f), summarized for the Desert, Semiarid, Mesic, Woodland-shrubland, and Forest ecosystem classes of our study. Extreme events in 2030–2100 were calculated from corresponding future values, capturing increasing future event magnitude (method 1)

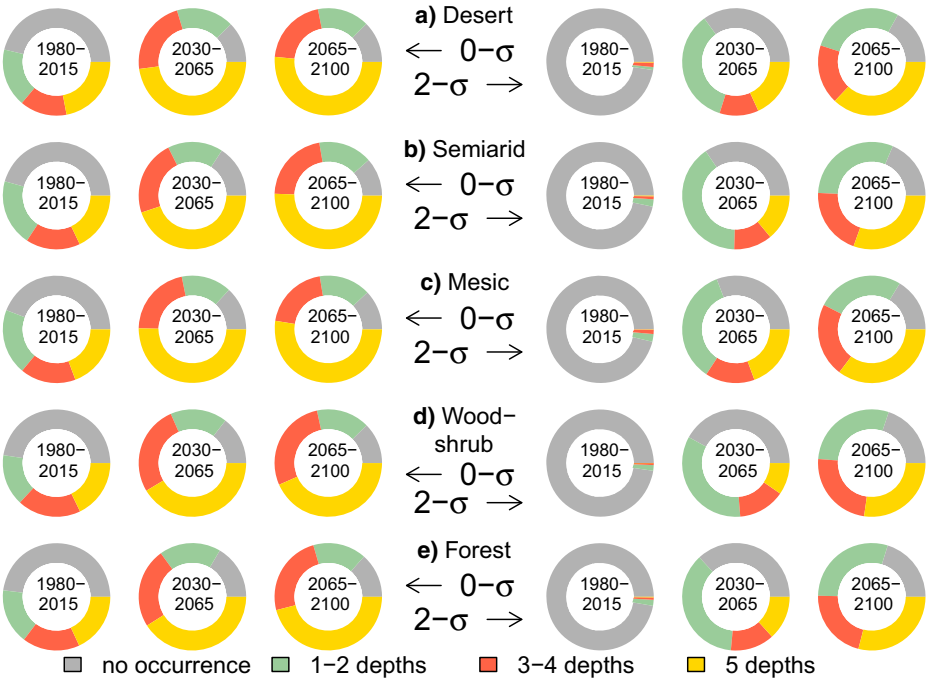

Fig. 4 Pie charts illustrating the proportion of months from April to October with co-occurring 0-σ or 2-σ extreme Ts events (0–100 cm; maximum 5 depths), summarized for the Desert, Semiarid, Mesic, Woodland-shrubland, and Forest ecosystem classes of our study. Summaries are presented for 1980–2015, 2030–2065, and 2065–2100 (CESM1-CAM5, RCP 8.5). Extreme events in 2030–2065 and 2065–2100 were calculated from 1980 to 2015 values (method 2)

In 2030–2065, the extreme Ta and Ts events (0–20 cm) will increase at the 0-σ level, whereas extreme Ts events at 50–100 cm will decrease (Fig. 6a; Supplementary Table 6). In 2065–2100, the frequency of these 0-σ extreme events will decrease, often below levels experienced in 1980–2015 (Fig. 6a). Declines in 0-σ extreme events will be offset by corresponding increases in the frequency of 2-σ extreme events, which will experience the greatest increases in frequency of occurrence (1980–2015: $\sim$ 0.9 events per decade; 2030–2065: $\sim$ 23 events per decade (+2600%); 2065–2100: $\sim$ 38 events (+4300%; Fig. 6b). These increases will be largest in June–July (not shown).

The monthly co-occurrence of extreme Ts events at multiple depths in the soil profile will also increase in the twenty-first century. In 1980–2015, $\sim$ 46% of months did not experience a 0-σ or 2-σ extreme event at any depth in the soil profile, and it was uncommon for a location to experience multiple extreme events in the same month (Fig. 4). In 2030–2065, $\sim$ 69% of months will experience extreme events at 3+ soil depths at the 0-σ level, and $\sim$ 45% of months will experience 0-σ extreme events throughout the soil profile (Fig. 4). Co-occurrence will further increase in 2065–2100, such that 2-σ extreme events will occur at 3+ depths in the majority (53%) of months (Fig. 4). The correlation between extreme Ta and Ts events will remain similar across twenty-first century time periods, suggesting that Ta influence on Ts will remain similar between past and future time periods (Supplementary Fig. 4).

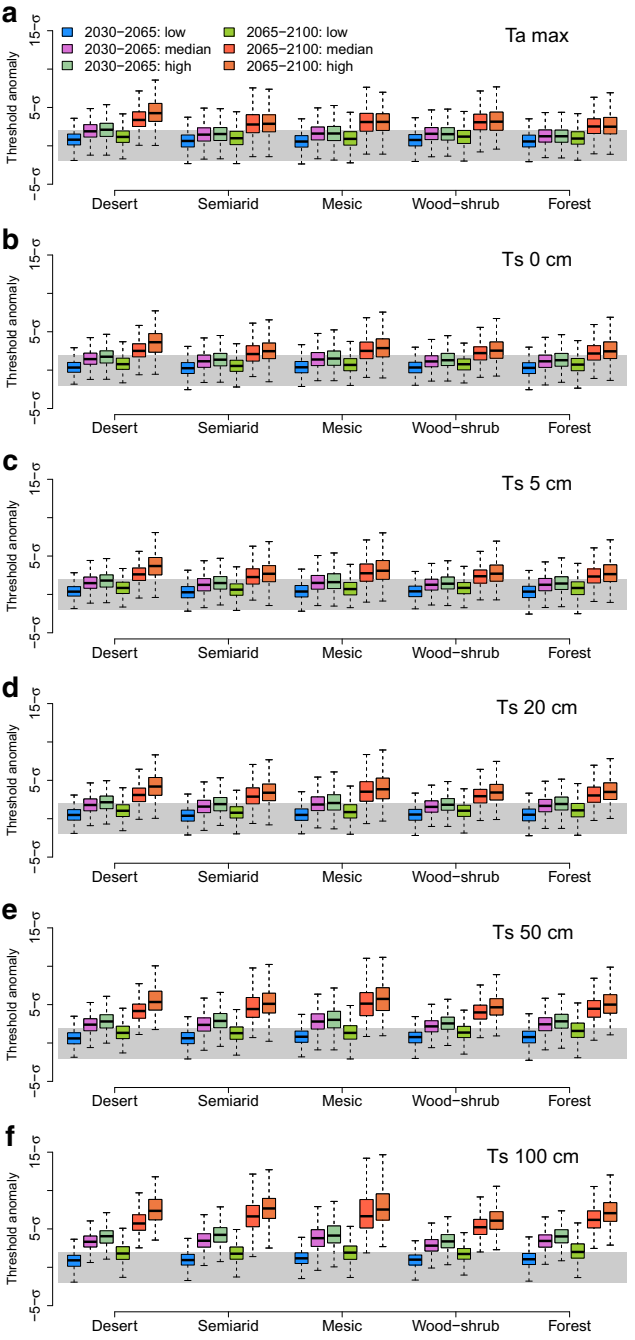

Fig. 5 Boxplots illustrating extreme event anomalies for 2030–2065 and 2065–2100. Extreme events in 2030–2065 and 2065–2100 were calculated from 1980 to 2015 values (illustrated with a grey bounding box; method 2). Values include the second-lowest GCM (inmcm4: the median of the 3 lowest future projection models: low), the median GCM (CESM-CAM5: the median of all 11 models: median), and the second-highest GCM (IPSL-CM5A-MR: the median of the 3 highest future projection models: high)

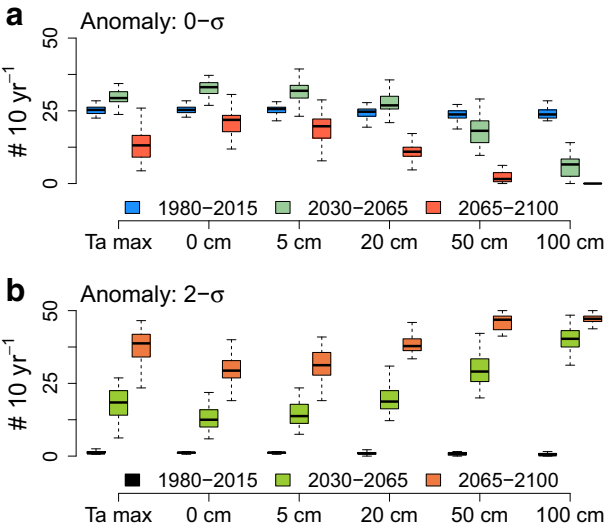

Fig. 6 Boxplots illustrating the frequency (# 10 year^{-1}) of months corresponding to 0-σ (panel a) and 2-σ (panel b) extreme events between 1980–2015, 2030–2065, and 2065–2100 (future values from CESM-CAM5: the median of all 11 models) for maximum air temperature (Ta max) and soil temperatures (0–100 cm depth). Boxplots include all study locations. Extreme events in 2030–2065 and 2065–2100 were calculated from 1980 to 2015 values (method 2)

5 Discussion

5.1 Extreme temperature events and climate change

Ta max was the primary variable correlated with Ts in the ecosystems of our study, and variables regulating temperature propagation at the soil surface (aboveground plant biomass) and belowground (soil clay content, bulk density, thermal conductivity) had sub-dominant influences (objective 1). This partially supports our hypothesis that the magnitude and occurrence of extreme Ts events lower in the soil profile is dampened compared to Ta and Ts in upper soil layers, as extreme Ts events were of higher magnitude and occurred more frequently at 0–20 cm than at 100 cm for all time periods (1980–2015, 2030–2065, 2065–2100). In refutation of our hypothesis, we did not find evidence of increased correlation between Ta and Ts over twenty-first century time periods (Supplementary Fig. 4). Future change to regional land-atmosphere interactions is expected to intensify climate extremes including drought and heat waves (Ukkola et al. 2018; Anderegg et al. 2019), and when combined with the results of our study suggest that local land-atmosphere interactions leading to altered temperature patterns may differ from those that occur across broad spatial scales.

We found that the threshold temperature values that designate extreme Ta and Ts events (method 1: higher magnitude assessed from future projections) will consistently exceed the magnitude of historical extreme events across all ecosystem classes, analysis locations, soil depths, and GCM futures. The largest increases in temperature extremes will occur for Ta and for Ts in upper soil layers, whereas the largest proportional increases by anomaly (not magnitude) will occur for Ts at 50–100-cm soil depths due to the relatively stable temperatures that these layers experienced historically (objective 2). The largest projected increases

in extreme Ta and Ts events by magnitude will occur in Semiarid, Mesic, and Wood-shrub ecosystems. In 2065–2100, Semiarid and Mesic ecosystems will experience similar extreme Ta and Ts events to those of Deserts in 1980–2015, and Wood-shrub ecosystems will experience extreme events exceeding those of Mesic and Semiarid ecosystems in 1980–2015. The distribution of 2-σ extreme events (method 2: future occurrence based on past patterns) will shift from occurring rarely in 1980–2015 to occurring in the majority of months in 2030–2065 and 2065–2100. These results portend to a substantial increase in the frequency of months with extreme high temperatures, and to the increasing co-occurrence of these events throughout the soil profile (objective 3). Forecasts for increasing Ta corroborate trends predicted by broader multimodel syntheses (IPCC 2013), and by the 11 GCMs used in this study. We conclude that the ecosystems of our study are likely to experience change to the occurrence and magnitude of temperature extremes that—like other predicted increases to global change drivers—have no contemporary analog.

5.2 Ecological and agricultural significance

The impacts of extreme Ts events could be realized across levels of biological organization (Jentsch and Beierkuhnlein 2008; Latimer and Zuckerberg 2019) and may interact with other driving climate variables to alter the range and persistence of many ecosystems (Thuiller et al. 2008). Considerable insight continues to be developed at the interface of climate and land-atmosphere interactions, especially the alteration of interactions between climate and the water cycle that can amplify or dampen water- and energy-driven processes across spatial and temporal scales (Brunsell and Gillies 2003; Anderegg et al. 2019). We postulate that increasing extreme Ts events could play an important role in shaping these interactions in the future. Yet, there is a substantial mismatch between the scales experienced by organisms and the scale at which climate data are collected and modeled (Potter et al. 2013). Multiple processes determine how broad-scale projections of environmental change relate to actual landscapes (Franklin et al. 2013). For example, some studies have shown that vegetation can play a major role in defining air temperature at local scales (De Frenne et al. 2013; Frey et al. 2016), implying that vegetation may support microrefugial conditions allowing species to persist through climate change (Dobrowski et al. 2015). Contrasting examples of this include the role of favorable landscape characteristics and sheltered microclimates for seedling survival in western US coniferous forests (Dobrowski et al. 2015; Urza et al. 2019), and enhancement of air temperatures by desert shrublands that limits the expansion and recovery of desert grasses (D'Odorico et al. 2010). We found that factors including aboveground plant biomass and physical soil characteristics had sub-dominant influences on Ts at our point-based simulation locations. It is likely that spatial variation in these factors—in addition to topography—plays an important role in Ts impacts to ecosystems. Better understanding of climate-landscape-ecosystem relationships and identification of the conditions that are meaningful for ecosystem processes are therefore among the most important components of forecasting ecological change.

Linking fine-scale insight on Ts change broadly across ecological regions will also be an important aspect of anticipating and preparing for the future. Of potential temperature-driven impacts to ecosystems, the influence of Ts on soil microbial activity, nutrient mineralization, and soil respiration is generally expected to decline at the high Ts values predicted in our study (Yuste et al. 2007; Hamdi et al. 2013). Yuste et al. (2007) found that short-duration (12 h) near-surface Ts extremes of 30–35 °C significantly reduced microbial activity and soil respiration in ecosystems similar to the Wood-shrub and Forest ecosystem

classes of our study, and Irina et al. (2019) found that decomposition in ecosystems similar to the Forests of our study declined with experimental warming from 15 to 25 °C. Extreme Ts has been found to have a greater impact on microbial activity during dry periods than impacts from water limitation, with severe die-offs of microbial communities occurring at 50 °C (Berard et al. 2011). Declines in biological rates of functioning at the soil surface and belowground would have deleterious impacts to ecosystem stability in dryland regions that are vulnerable to desertification during sustained periods of low net primary production (D'Odorico et al. 2013), and the consequences of degraded soil microbial communities may be important at regional and global scales (Hamdi et al. 2013; Rodriguez-Caballero et al. 2018). The properties of change to Ts and extreme Ts events that we observed in our study suggests that future impacts biological functioning at the soil surface and belowground could be even more severe than predictions based solely on change to Ta.

Increasing Ts may also have severe impacts to aboveground ecosystem processes. In a semiarid ecosystem similar to those of our study, James et al. (2019) suggest a 30% decline in grass seedling recruitment at a level of elevated Ts that is of lower magnitude than the values we predicted for the coming century. In Forest ecosystems, it has long been known that extreme Ts reduces tree seedling germination and survival (Petrie et al. 2016), and values initiating mortality are again lower than values predicted by our study. Across North American forests, high temperature extremes early in the growing season may lead to substantial but divergent influences on carbon exchanges and changing ecosystem sensitivity to drought (Xu et al. 2019). Increasing Ts could promote the expansion of desert shrubs at the expense of herbaceous grasses (D'Odorico et al. 2010; He et al. 2015), yet Ts increases may also have deleterious impacts on the ecophysiology of these expanding shrub species (Hamerlynck et al. 2000), potentially leading to conditions that do not favor either shrubs or grasses. In Mesic ecosystems, we postulate that extreme Ts events could limit projected increases in grassland productivity due to increasing growing season length by reducing plant photosynthesis and net primary production later in the growing season (Hufkens et al. 2016). More broadly, the magnitude of temperature extremes predicted for the twenty-first century may exceed the thermal tolerance limits of plant leaf metabolism (O'Sullivan et al. 2017), and the thermal tolerance limits of many organisms (Buckley and Huey 2016). These examples comprise only a subset of potential ecosystem consequences of increasing Ts. We propose that future ecological change may be best anticipated by determining where and to what magnitude increasing temperatures will approach and exceed the stress tolerance of key species, and incorporating this information into ongoing research on species demography, distributions, and community dynamics (Kearney and Porter 2009; Dell et al. 2011).

Although we did not evaluate agricultural systems in our study, our study locations overlap geographically with important agricultural regions. Extreme Ts events are predicted to constrain the viability of rainfed agriculture (Bradford et al. 2017) and may have broad impacts on crop viability. In a review paper, Porter and Semenov (2005) found similar relationships in the response of multiple crop types to increasing temperatures, with severe declines in productivity and food quality at Ta values exceeding critical ranges (often 30–35 °C). In Brazil, Noia Junior et al. (2018) found that extreme soil temperature pulses of 30–40 °C significantly reduced plant carboxylation and root production, and increased leaf temperatures. Our results show that Ta values exceeding 35 °C will become increasingly common in agricultural systems in coming decades, and will co-occur alongside extreme Ts events that also exceed 35 °C. It is therefore urgent to understand to what degree increasing and co-occurring extreme Ta and Ts events could impact agricultural productivity and food quality.

5.3 Future directions in extreme temperatures

Although the study locations and ecosystem classes of our study do not represent all of the diverse ecosystems located in our study region, they provide insight on the future magnitude and occurrence of extreme temperatures that ecosystems in the central and western USA will experience in coming decades. Our research illustrates the changing distribution of extreme events towards the 0-σ and 2-σ level of events at the monthly time step, which suggests an increasing duration of high temperature periods but does not resolve these increases directly. Future projections focused on event duration, perhaps based on temporal exceedance above locally determined thresholds (similar to those of our study), would provide additional insight on the multiple properties of extreme temperatures.

Variability in winter climate and especially minimum daily temperatures often has effects extending into other times of year (Schlaepfer et al. 2012; Petrie et al. 2015; Collins et al. 2017). Increasing winter temperatures are driving notable changes in the rate and magnitude of soil decomposition and greenhouse gas emissions in high-latitude ecosystems (Tian et al. 2016; Poeplau et al. 2017). We did not evaluate minimum temperatures in this study, in part due to our interest in high growing season temperatures, and due to the lack of snow data for our study locations. Of winter processes influencing Ts, soil freezing-thawing and snowpack insulation are especially important because they decouple surface and belowground temperatures from Ta fluctuations (Koren et al. 1999). Both of these processes are simulated by SOILWAT2, but we were unable to validate them for our study locations because we did not have field observations of snowpack, and freeze-thaw dynamics are difficult to capture with soil temperature and moisture sensors. We propose that change to minimum temperatures and minimum temperature extremes deserves more attention (see Wheeler et al. 2014 and Choler 2018 for examples in cooler regions), specifically through research that links detailed soil and snowpack dynamics measured in the field to broader scale estimates from Land Surface Models (LSMs) and spatial data products (see Henry et al. 2018 for an example).

6 Conclusions

We validated surface and soil temperature (Ts: 0–100-cm depth) simulations in the SOILWAT2 model for 29 locations comprising 5 ecosystem types in the central and western USA, and explored simulations of Ta and Ts change over 1980–2015, 2030–2065, and 2065–2100 time periods. Our analyses focused on temperature extremes, quantified from standard deviations above the mean. We found that, across the ecosystem types of our study, future increases to the frequency and magnitude of Ts extreme events have no contemporary analog. Increases in extreme Ts events will often exceed +10 °C at 0–20 cm by 2065–2100, and at 0–100 cm will often exceed 5.0 standard deviations above 1980–2015 values. By 2065–2100, the majority of months will experience extreme events that co-occur at 0–100 cm, which did not occur in 1980–2015. Our results suggest that there is a pressing need to incorporate belowground temperature change in forecasts of climate-driven ecological change for the twenty-first century.

Funding Portions of this study were funded by a grant from the USDA Forest Service, Western Wildland Environmental Threat Assessment Center.

Data availability No new data were created or analyzed in this study. Model simulation outputs that support the findings of this study are available from the corresponding author upon reasonable request.

Code availability SOILWAT2 documentation and code is available on github (see Schlaepfer and Andrews 2019 and Schlaepfer and Murphy 2019).

Compliance with ethical standards

Conflict of interest The authors declare that they have no conflict of interest.

Disclaimer Any use of trade, product, or firm names is for descriptive purposes only and does not imply endorsement by the US Government.

Supplementary Information The online version contains supplementary material available at (https://doi.org/10.1007/s10584-020-02944-7).

Appendix

We used the peak over threshold (POT) technique of Coelho et al. (2008) to calculate monthly extreme temperature thresholds from daily values of Ta and Ts. This analysis is conducted for a timeseries of each month individually (e.g., all days in January from 1980 to 2015). We calculated the monthly extreme temperature threshold using the following steps:

Step 1. Calculate the 5-year floating mean from daily values. Using the 5-year floating mean results in an analysis window that is 4 years shorter than the time period length. For example, 1980–2015 has a floating mean for 1982–2013.

Step 2. Rank the daily values in each month (January, 1983, for example) that are above the corresponding floating mean temperature value from highest to lowest (x = a vector of ranked daily temperature values).

Step 3. Multiply the number of daily values in x by 0.05 (Obs = number of observations in x multiplied by 0.05).

Step 4. If $Obs < 1.0$, there is no extreme threshold value for the corresponding month, and therefore no extreme event.

Step 5. If $Obs \geq 1.0$, the extreme threshold value for the corresponding month is the Obs+1th value in x. This value is assigned as a monthly extreme event.

References

Alster C, von Fischer J, Allison S, Treseder K (2020) Embracing a new paradigm for temperature sensitivity of soil microbes. Glob Change Biol. https://doi.org/10.1111/gcb.15053

Anderegg W, Trugman A, Bowling D, Salvucci G, Tuttle S (2019) Plant functional traits and climate influence drought intensification and land–atmosphere feedbacks. Proc Natl Acad Sci USA 116:14071–14076. https://doi.org/10.1073/pnas.1904747116

Barron-Gafford GA, Scott RL, Jenerette GD, Hamerlynck EP, Huxman TE (2012) Temperature and precipitation controls over leaf- and ecosystem-level CO2 flux along a woody plant encroachment gradient. Glob Change Biol 18:1389–1400. https://doi.org/10.1111/j.1365-2486.2011.02599.x

Bell D, Bradford J, Lauenroth W (2014) Early indicators of change: divergent climate envelopes between tree life stages imply range shifts in the western United States. Glob Ecol Biogeogr 23:168–180. https://doi.org/10.1111/geb.12109

Belnap J (2002) Nitrogen fixation in biological soil crusts from southeast Utah, USA. Biol Fertil Soils 35:128–135. https://doi.org/10.1007/s00374-002-0452-x

Berard A, Bouchet T, Sevenier G, Pablo A, Gros R (2011) Resilience of soil microbial communities impacted by severe drought and high temperature in the context of Mediterranean heat waves. Eur J Soil Biol 47:333–342. https://doi.org/10.1016/j.ejsobi.2011.08.004

Betts R, Cox P, Woodward F (2000) Simulated responses of potential vegetation to doubled-CO2 climate change and feedbacks on near-surface temperature. Glob Ecol Biogeogr 9:171–180. https://doi.org/10.1046/j.1365-2699.2000.00160.x

Bradford J, Bell D (2017) A window of opportunity for climate-change adaptation: easing tree mortality by reducing forest basal area. Front Ecol Environ 15:11–17. https://doi.org/10.1002/fee.1445

Bradford J, Schlaepfer D, Lauenroth W (2014a) Ecohydrology of adjacent sagebrush and Lodgepole pine ecosystems: the consequences of climate change and disturbance. Ecosystems 17:590–605. https://doi.org/10.1007/s10021-013-9745-1

Bradford J, Schlaepfer D, Lauenroth W, Burke I (2014b) Shifts in plant functional types have time-dependent and regionally variable impacts on dryland ecosystem water balance. J Ecol 102:1408–1418. https://doi.org/10.1111/1365-2745.12289

Bradford J, Schlaepfer D, Lauenroth W, Yackulic C, Duniway M, Hall S, Jia G, Jamiyansharav K, Munson S, Wilson S, Tietjen B (2017) Future soil moisture and temperature extremes imply expanding suitability for rainfed agriculture in temperate drylands. Sci Rep 7:12923. https://doi.org/10.1038/s41598-017-13165-x

Bradford M, Wieder W, Bonan G, Fierer N, Raymond P, Crowther T (2016) Managing uncertainty in soil carbon feedbacks to climate change. Nat Clim Change 6:751–758. https://doi.org/10.1038/NCLIMATE3071

Brunsell NA, Gillies RR (2003) Scale issues in land-atmosphere interactions: implications for remote sensing of the surface energy balance. Agric For Meterol 117:203–221. https://doi.org/10.1016/S0168-1923(03)00064-9

Buckley L, Huey R (2016) Temperature extremes: geographic patterns, recent changes, and implications for organismal vulnerabilities. Glob Change Biol 22:3829–3842. https://doi.org/10.1111/gcb.13313

Burnham K, Anderson D (2002) Model selection and multimodel inference, vol 1. Springer, New York

Burnham K, Anderson D (2004) Multimodel inference—understanding AIC and BIC in model selection. Sociol Methods Res 33:261–304. https://doi.org/10.1177/0049124104268644

Chatfield C (1995) Model uncertainty, data mining and statistical-inference. J R Stat Soc Ser A - Stat Soc 158:419–466. https://doi.org/10.2307/2983440

Choler P (2018) Winter soil temperature dependence of alpine plant distribution: implications for anticipating vegetation changes under a warming climate. Perspect Plant Ecol Evol System 30:6–15. https://doi.org/10.1016/j.ppees.2017.11.002

Chung Y, Thornton B, Dettweiler-Robinson E, Rudgers J (2019) Soil surface disturbance alters cyanobacterial biocrusts and soil properties in dry grassland and shrubland ecosystems. Plant Soil 441:147–159. https://doi.org/10.1007/s11104-019-04102-0

Coelho CAS, Ferro CAT, Stephenson DB (2008) Methods for exploring spatial and temporal variability of extreme events in climate data. J Clim 21:2072–2092. https://doi.org/10.1175/2007JCLI1781.1

Collins S, Ladwig L, Petrie M, Jones S, Mulhouse J, Thibault J, Pockman W (2017) Press–pulse interactions: effects of warming, N deposition, altered winter precipitation, and fire on desert grassland community structure and dynamics. Glob Change Biol 45, in press. https://doi.org/10.1111/gcb.13493

Darrouzet-Nardi A, Reed S, Grote E, Belnap J (2015) Observations of net soil exchange of CO2 in a dryland show experimental warming increases carbon losses in biocrust soils. Biogeochemistry 126:363–378. https://doi.org/10.1007/s10533-015-0163-7

De Frenne P, Rodriguez-Sanchez F, Coomes D, Baeten L, Verstraeten G, Vellend M, Bernhardt-Roemermann M, Brown C, Brunet J, Cornelis J, Decocq G, Dierschke H, Eriksson O, Gilliam F, Hedl R, Heinken T, Hermy M, Hommel P, Jenkins M, Kelly D, Kirby K, Mitchell F, Naaf T, Newman M, Peterken G, Petrik P, Schultz J, Sonnier G, Van Calster H, Waller D, Walther G, White P, Woods K, Wulf M, Graae B, Verheyen K (2013) Microclimate moderates plant responses to macroclimate warming. Proc Natl Acad Sci USA 110:18561–18565. https://doi.org/10.1073/pnas.1311190110

Dell A, Pawar S, Savage V (2011) Systematic variation in the temperature dependence of physiological and ecological traits. Proc Natl Acad Sci USA 108:10591–10596. https://doi.org/10.1073/pnas.1015178108

Diffenbaugh N, Pal J, Trapp R, Giorgi F (2005) Fine-scale processes regulate the response of extreme events to global climate change. Proc Natl Acad Sci USA 102:15774–15778. https://doi.org/10.1073/pnas.0506042102

Dobrowski S, Swanson A, Abatzoglou J, Holden Z, Safford H, Schwartz M, Gavin D (2015) Forest structure and species traits mediate projected recruitment declines in western US tree species. Glob Ecol Biogeogr 24:917–927. https://doi.org/10.1111/geb.12302

D'Odorico P, Bhattachan A, Davis KF, Ravi S, Runyan CW (2013) Global desertification: drivers and feedbacks. Adv Water Resour 51:326–344. https://doi.org/10.1016/j.advwatres.2012.01.013

D'Odorico P, Fuentes J, Pockman W, Collins S, He Y, Medeiros J, DeWekker S, Litvak M (2010) Positive feedback between microclimate and shrub encroachment in the northern Chihuahuan Desert. Ecosphere 1:1–11

Duveiller G, Fasbender D, Meroni M (2015) Revisiting the concept of a symmetric index of agreement for continuous datasets. Sci Rep 6:1–14. https://doi.org/10.1038/srep19401

Eitzinger J, Parton W, Hartman M (2000) Improvement and validation of a daily soil temperature submodel for freezing/thawing periods. Soil Sci 165:525–534

Franklin J, Davis FW, Ikegami M, Syphard AD, Flint LE, Flint AL, Hannah L (2013) Modeling plant species distributions under future climates: how fine scale do climate projections need to be? Glob Change Biol 19:473–483. https://doi.org/10.1111/gcb.12051

Frey S, Hadley A, Johnson S, Schulze M, Jones J, Betts M (2016) Spatial models reveal the microclimatic buffering capacity of old-growth forests. Sci Adv 2: UNSP e1501392. https://doi.org/10.1126/sciadv.1501392

Garcia-Suarez A, Butler C (2006) Soil temperatures at Armagh Observatory, Northern Ireland, from 1904 to 2002. Int J Climatol 26:1075–1089. https://doi.org/10.1002/joc.1294

Gutzler D, Robbins T (2011) Climate variability and projected change in the western United States: regional downscaling and drought statistics. Clim Dyn 37:835–849. https://doi.org/10.1007/s00,382-010-0838-7

Hamdi S, Moyano F, Sall S, Bernoux M, Chevallier T (2013) Synthesis analysis of the temperature sensitivity of soil respiration from laboratory studies in relation to incubation methods and soil conditions. Soil Biol Biochem 115–126. https://doi.org/10.1016/j.soilbio.2012.11.012

Hamerlynck E, Huxman T, Loik M, Smith S (2000) Effects of extreme high temperature, drought and elevated CO2 on photosynthesis of the Mojave Desert evergreen shrub, Larrea tridentata. Plant Ecol 148:183–193. https://doi.org/10.1023/A:1009896111405

He Y, D'Odorico P, De Wekker S (2015) The role of vegetation-microclimate feedback in promoting shrub encroachment in the northern Chihuahuan desert. Glob Change Biol 21:2141–2154. https://doi.org/10.1111/gcb.12856

Henn B, Raleigh M, Fisher A, Lundquist J (2013) A comparison of methods for filling gaps in hourly near-surface air temperature data. J Hydrometeorol 14:929–945. https://doi.org/10.1175/JHM-D-12-027.1

Henry H, Abedi M, Alados C, Beard K, Fraser L, Jentsch A, Kreyling J, Kulmatiski A, Lamb E, Sun W, Vankoughnett M, Venn S, Werner C, Beil I, Blindow I, Dahlke S, Effinger A, Garris H, Gartzia M, Gebauer T, Arfin Khan M, Malyshev A, Morgan J, Nock C, Paulson J, Pueyo Y, Stover H, Yang X (2018) Increased soil frost versus summer drought as drivers of plant biomass responses to reduced precipitation: results from a globally coordinated field experiment. Ecosystems 21:1432–1444. https://doi.org/10.1007/s10021-018-0231-7

Hufkens K, Keenan T, Flanagan L, Scott R, Bernacchi C, Joo E, Brunsell N, Verfaillie J, Richardson A (2016) Productivity of North American grasslands is increased under future climate scenarios despite rising aridity. Nat Clim Change 6:710–714. https://doi.org/10.1038/NCLIMATE2942

IPCC (2013) Climate change 2013: I the physical science basis. Cambridge University Press, London

Irina K, Ekaterina T, Ruzalia V, Ekaterina V, Marina V (2019) Effect of temperature on litter decomposition, soil microbial community structure and biomass in a mixed-wood forest in European Russia. Curr Sci 116:765–772. https://doi.org/10.18520/cs/v116/i5/765-772

James J, Sheley R, Leger E, Adler P, Hardegree S, Gornish E, Rinella M (2019) Increased soil temperature and decreased precipitation during early life stages constrain grass seedling recruitment in cold desert restoration. J Appl Ecol, press. https://doi.org/10.1111/1365-2664.13508

Jentsch A, Beierkuhnlein C (2008) Research frontiers in climate change: effects of extreme meteorological events on ecosystems. Comptes Rendus Geosci 340:621–628. https://doi.org/10.1016/j.crte.2008.07.002

Julien Y, Sobrino J (2009) Global land surface phenology trends from GIMMS database. Int J Remote Sens 13:3495–3513

Katz R, Brown B (1992) Extreme events in a changing climate—variability is more important than averages. Clim Change 21:289–302. https://doi.org/10.1007/BF00139728

Kearney M, Porter W (2009) Mechanistic niche modelling: combining physiological and spatial data to predict species' ranges. Ecol Lett 12:334–350. https://doi.org/10.1111/j.1461-0248.2008.01277.x

King A, Black M, Min S, Fischer E, Mitchell D, Harrington L, Perkins-Kirkpatrick S (2016) Emergence of heat extremes attributable to anthropogenic influences. Geophys Res Lett 43:3438–3443. https://doi.org/10.1002/2015GL067448

Knutti R, Masson D, Gettelman A (2013) Climate model genealogy: generation CMIP5 and how we got there. Geophys Res Lett 40:1194–1199

Koren V, Schaake K, Duan Q, Chen F, Baker J (1999) A parameterization of snowpack and frozen ground intended for NCEP weather and climate models. J Geophys Res 104:19569–19585

Latimer C, Zuckerberg B (2019) How extreme is extreme? Demographic approaches inform the occurrence and ecological relevance of extreme events. Ecol Monographs 89:UNSP e01385. https://doi.org/10.1002/ecm.1385

Maurer E, Wood A, Adam J, Lettenmaier D, Nijssen B (2002) A long-term hydrologically based dataset of land surface fluxes and states for the conterminous United States. J Clim 15:3237–3251. https://doi.org/10.1175/1520-0442(2002)015<3237:ALTHBD>2.0.CO;2

Maurer E, Brekke L, Pruitt T, Duffy P (2007) Fine-resolution climate projections enhance regional climate change impact studies. Eos Trans AGU 88:504

Mora C, Dousset B, ICaldwell I, Powell F, Geronimo R, Bielecki C, Counsell C, Dietrich B, Johnston E, Louis L, Lucas M, McKenzie M, Shea A, Tseng H, Giambelluca T, Leon L, Hawkins E, Trauernicht C (2017) Global risk of deadly heat. Nat Clim Change 7:501–506. https://doi.org/10.1038/nclimate3322

Moran M, Peters D, McClaran M, Nichols M, Adams M (2008) Long-term data collection at USDA experimental sites for studies of ecohydrology. Ecohydrology 1:377–393. https://doi.org/10.1002/eco.24

Noia Junior R, do Amaral G, Macedo Pezzopane J, Toledo J, Teixeira Xavier T (2018) Ecophysiology of C3 and C4 plants in terms of responses to extreme soil temperatures. Theor Exp Plant Physiol 30:261–274. https://doi.org/10.1007/s40626-018-0120-7

O'Sullivan O, Heskel M, Reich P, Tjoelker M, Weerasinghe L, Penillard A, Zhu L, Egerton J, Bloomfield K, Creek D, Bahar N, Griffin K, Hurry V, Meir P, Turnbull M, Atkin O (2017) Thermal limits of leaf metabolism across biomes. Glob Change Biol 23:209–223. https://doi.org/10.1111/gcb.13477

Petrie M, Pockman W, Pangle R, Limousin J, Plaut J, McDowell N (2015) Winter climate change promotes altered spring growing season in piñon pine-juniper woodlands. Agric For Meteorol 214–215:357–368. https://doi.org/10.1016/j.agrformet.2015.08.269

Petrie M, Bradford J, Hubbard R, Lauenroth W, Andrews C, Schlaepfer D (2017) Climate change may restrict dryland forest regeneration in the 21st century. Ecology 90:1548–1559. https://doi.org/10.1002/ecy.1791

Petrie M, Wildeman A, Bradford J, Hubbard R, Lauenroth W (2016) A review of precipitation and temperature control on seedling emergence and establishment for ponderosa and lodgepole pine forest regeneration. For Ecol Manag 361:328–338. https://doi.org/10.1016/j.foreco.2015.11.028

Pineiro G, Perelman S, Guerschman J, Paruelo J (2008) How to evaluate models: observed vs. predicted or predicted vs. observed? Ecol Model 216:316–322. https://doi.org/10.1016/j.ecolmodel.2008.05.006

Poeplau C, Katterer T, Leblans N, Sigurdsson B (2017) Sensitivity of soil carbon fractions and their specific stabilization mechanisms to extreme soil warming in a subarctic grassland. Glob Change Biol 23:1316–1327. https://doi.org/10.1111/gcb.13491

Porter J, Semenov M (2005) Crop responses to climatic variation. Philos Trans R Soc B - Biol Sci 360:2021–2035. https://doi.org/10.1098/rstb.2005.1752

Potter K, Woods H, Pincebourde S (2013) Microclimatic challenges in global change biology. Glob Change Biol 19:2932–2939. https://doi.org/10.1111/gcb.12257

Qian B, Gregorich E, Gameda S, Hopkins D, Wang X (2011) Observed soil temperature trends associated with climate change in Canada. J Geophys Res - Atmos 116. https://doi.org/10.1029/2010JD015012

R Development Core Team (2019) R: a language and environment for statistical computing. R Foundation for Statistical Computing, Vienna, Austria, ISBN 3-900051-07-0, http://www.R-project.org

Ratajczak Z, Churchill A, Ladwig L, Taylor J, Collins S (2019) The combined effects of an extreme heatwave and wildfire on tallgrass prairie vegetation. J Veg Sci 30:687–697. https://doi.org/10.1111/jvs.12750

Reichstein M, Bahn M, Ciais P, Frank D, Mahecha M, Seneviratne S, Zscheischler J, Beer C, Buchmann N, Frank D, Papale D, Rammig A, Smith P, Thonicke K, van der Velde M, Vicca S, Walz A, Wattenbach M (2013) Climate extremes and the carbon cycle. Nature 500:287–295. https://doi.org/10.1038/nature12350

Rodriguez-Caballero E, Belnap J, Buedel B, Crutzen P, Andreae M, Poeschl U, Weber B (2018) Dryland photoautotrophic soil surface communities endangered by global change. Nat Geosci 11:185+. https://doi.org/10.1038/s41561-018-0072-1

Rudgers J, Dettweiler-Robinson E, Belnap J, Green L, Sinsabaugh R, Young K, Cort C, Darrouzet-Nardi A (2018) Are fungal networks key to dryland primary production? Am J Bot 105:1783–1787. https://doi.org/10.1002/ajb2.1184

Rupp D, Abatzoglou J, Hegewisch K, Mote P (2013) Evaluation of CMIP5 20th century climate simulations for the Pacific Northwest USA. J Geophys Res - Atmospheres 118:10884–10906. https://doi.org/10.1002/jgrd.50843

Sarle W (1995) Stopped training and other remedies for overfitting. In: Proceedings of the symposium on the interface of computing science and statistics, vol 27, pp 1–10
Schlaepfer D, Andrews C (2019) rSFSW2: simulation framework for SOILWAT2. R package version 3.2.0, https://github.com/DrylandEcology/rSFSW2
Schlaepfer D, Murphy R (2019) rSOILWAT2: an ecohydrological ecosystem-scale water balance simulation model. R package version 2.5.0. https://github.com/DrylandEcology/rSOILWAT2
Schlaepfer D, Lauenroth W, Bradford J (2012) Consequences of declining snow accumulation for water balance of mid-latitude dry regions. Glob Change Biol 18:1988–1997. https://doi.org/10.1111/j.1365-2486.2012.02642.x
Schlaepfer D, Bradford J, Lauenroth W, Munson S, Tietjen B, Hall S, Wilson S, Duniway M, Jia G, Pyke D, Lkhagva A, Jamiyansharav K (2017) Climate change reduces extent of temperate drylands and intensifies drought in deep soils. Nat Commun 8. https://doi.org/10.1038/ncomms14196
Selig E, Casey K, Bruno J (2010) New insights into global patterns of ocean temperature anomalies: implications for coral reef health and management. Glob Ecol Biogeogr 19:397–411. https://doi.org/10.1111/j.1466-8238.2009.00522.x
Soil Survey Staff (2016) U.S. General Soil Map (STATSGO2). Natural Resources Conservation Service, United States Department of Agriculture, Available online at http://sdmdataaccess.nrcs.usda.gov/. Accessed 2016
Svilicic P, Vucetic V, Filic S, Smolic A (2016) Soil temperature regime and vulnerability due to extreme soil temperatures in Croatia. Theor Appl Climatol 126:247–263. https://doi.org/10.1007/s00704-015-1558-z
Thuiller W, Albert C, Araujo M, Berry P, Cabeza M, Guisan A, Hickler T, Midgely G, Paterson J, Schurr F, Sykes M, Zimmermann N (2008) Predicting global change impacts on plant species' distributions: future challenges. Perspect Plant Ecol Evol System 9:137–152. https://doi.org/10.1016/j.ppees.2007.09.004
Tian H, Lu C, Ciais P, Michalak A, Canadell J, Saikawa E, Huntzinger D, Gurney K, Sitch S, Zhang B, Yang J, Bousquet P, Bruhwiler L, Chen G, Dlugokencky E, Friedlingstein P, Melillo J, Pan S, Poulter B, Prinn R, Saunois M, Schwalm C, Wofsy S (2016) The terrestrial biosphere as a net source of greenhouse gases to the atmosphere. Nature 531:225+. https://doi.org/10.1038/nature16946
Tohver I, Hamlet A, Lee S-Y (2014) Impacts of 21st-century climate change on hydrologic extremes in the Pacific Northwest region of North America. J Am Water Resour Assoc 50:1461–1476
Ukkola A, Pitman A, Donat M, Kauwe M, Angelil O (2018) Evaluating the contribution of land-atmosphere coupling to heat extremes in CMIP5 models. Geophys Res Lett 45:9003–9012. https://doi.org/10.1029/2018GL079102
Urza A, Weisberg P, Chambers J, Sullivan B (2019) Shrub facilitation of tree establishment varies with ontogenetic stage across environmental gradients. New Phytol 223:1795–1808. https://doi.org/10.1111/nph.15957
Wenger S, Olden J (2012) Assessing transferability of ecological models: an underappreciated aspect of statistical validation. Methods Ecol Evol 3:260–267. https://doi.org/10.1111/nph.15957
Wheeler J, Hoch G, Cortes A, Sedlacek J, Wipf S, Rixen C (2014) Increased spring freezing vulnerability for alpine shrubs under early snowmelt. Oecologia 175:219–229. https://doi.org/10.1007/s00442-013-2872-8
Whitney K, Vivoni E, Duniway M, Bradford J, Reed S, Belnap J (2017) Ecohydrological role of biological soil crusts across a gradient in levels of development. Ecohydrology 10:e1875. https://doi.org/10.1002/eco.1875
Williams AP, Allen CD, Macalady AK, Griffin D, Woodhouse CA, Meko DM, Swetnam TW, Rauscher SA, Seager R, Grissino-Mayer HD, Dean JS, Cook ER, Gangodagamage C, Cai M, McDowell NG (2013) Temperature as a potent driver of regional forest drought stress and tree mortality. Nat Clim Change 3:292–297. https://doi.org/10.1038/NCLIMATE1693
Xu B, Arain M, Black T, Law B, Pastorello G, Chu H (2019) Seasonal variability of forest sensitivity to heat and drought stresses: a synthesis based on carbon fluxes from North American forest ecosystems. Glob Change Biol, in press. https://doi.org/10.1111/gcb.14843
Yuste J, Baldocchi D, Gershenson A, Goldstein A, Misson L, Wong S (2007) Microbial soil respiration and its dependency on carbon inputs, soil temperature and moisture. Glob Change Biol 13:2018–2035. https://doi.org/10.1111/j.1365-2486.2007.01415.x

Affiliations

M. D. Petrie[1] · J. B. Bradford[2] · W. K. Lauenroth[3] · D. R. Schlaepfer[2,3,4] · C. M. Andrews[2] · D. M. Bell[5]

1 School of Life Sciences, University of Nevada Las Vegas, Las Vegas, NV, USA
2 US Geological Survey, Southwest Biological Science Center, Flagstaff, AZ, USA
3 School of Forestry and Environmental Studies, Yale University, New Haven, CT, USA
4 Center for Adaptable Western Landscapes, Northern Arizona University, Flagstaff, AZ, USA
5 Pacific Northwest Research Station, USDA Forest Service, Corvallis, OR, USA